ELSEVIER

Cement & Concrete Composites 23 (2001) 411–417

Cement & Concrete Composites

www.elsevier.com/locate/cemconcomp

Interfacial shear transfer of RC beams strengthened by bonded composite plates

J.Q. Ye *

School of Civil Engineering, University of Leeds, Leeds, LS2 9JT, UK

Received 14 February 2000; accepted 14 February 2001

Abstract

In this paper an analytical method is proposed to predict the distributions of interfacial shear stress in concrete beams strengthened by composite plates. Non-linear behaviour of concrete under compression is considered in the analysis. The solutions show significant shear stress concentration near the cut-off end of plates. A parametrical study is carried out to show the effects of some design variables, e.g., thickness of adhesive layer, material properties and the distance from support to cut-off end of bonded plates. © 2001 Elsevier Science Ltd. All rights reserved.

Keywords: Concrete beam; Composite plate; Shear; Stress concentration; Strengthening

1. Introduction

As a nation's infrastructure ages, the number of deficient structures continues to grow. Based on recent bridge management statistics, a significant number of reinforced and prestressed concrete bridges in the EU require maintenance, repairs and strengthening. This problem is not confined only to the EU but also to other areas of the world. Because of the prohibitive cost of replacing all of the structures, governments and private sectors across the world are looking for new technologies and cost-effective solutions. Advanced composite materials have been identified as one of the best materials that have a number of unique advantages when they are used in civil engineering.

Using fibre-reinforced composite (FRP) plates as reinforcements to strengthen/repair deteriorated concrete structures has been proven to be a quick and economic method currently in use [3]. Because the plates are externally bonded to concrete, it is also realised that the bond at the interface between concrete and composite reinforcements has significant impact on the overall performance of a strengthened structural member. Strong bonding at the interface, although essential for efficient stress transfer, generally leads to an unstable catastrophic failure with cracks propagating right through the reinforcement (transverse cracking) and very limited energy absorption capacity. In contrast, weak interface bonding allows the toughening mechanisms to occur more extensively through longitudinal splitting. Therefore, the capacity of load transfer will be reduced and longer concrete crack spacing and crack width will be developed. Obviously, a better understanding of the stress transfer at interfaces may provide useful information and help designers select the best possible adhesive and composite materials. Extensive research has been done over last few years both experimentally, e.g. [1,6–8] and analytically or numerically, e.g. [2,4,9–12]. However, to the author's best knowledge, numerical results dealing with flexural interfaces and non-linear behaviour of concrete have not been found in the literature.

This paper presents some results in this area. An analytical and iterative method is used to investigate shear stress transfer at interfaces of concrete beams strengthened by FRP composite plates. A non-linear strain–stress relation is used for the concrete in compression. The steel rebars and the composite plate are assumed to be elastic–ideally plastic and linear elastic, respectively. Numerical results are obtained and compared with the results from alternative methods. Further results are presented to show the effects of thickness of adhesive layers, material properties of FRP plates and distances from support to the cut-off end of bonded plates.

* Fax: +44-0113-2332265.
E-mail address: j.ye@leeds.ac.uk (J.Q. Ye).

PII: S0958-9465(01)00015-4

2. Constitutive laws

The stress–strain relation of concrete in compression is assumed to follow Hognestad's idealised stress–strain curve [5] and shown in Fig. 1.

The relation of compressive stress and strain is given as

$$\begin{aligned}\sigma_c &= f_c''\left[\frac{2\varepsilon_c}{\varepsilon_0} - \left(\frac{\varepsilon_c}{\varepsilon_0}\right)^2\right] \quad 0 \leqslant \varepsilon_c \leqslant \varepsilon_0,\\ \sigma_c &= f_c''\left[1 - \frac{0.15}{0.004 - \varepsilon_0}(\varepsilon_c - \varepsilon_0)\right] \quad \varepsilon_0 \leqslant \varepsilon_c < 0.003,\end{aligned} \tag{1}$$

where σ_c and ε_c are compressive stress and strain in concrete, respectively; $f_c'' = \zeta f_c'$, where f_c' is concrete compressive strength, f_c'' is maximum compressive stress in concrete; ε_0 is the strain in concrete at maximum stress and $\varepsilon_0 = 2f_c''/E_c$, where E_c is the modulus of elasticity of concrete.

The stress–strain relation of steel rebars is assumed to be elastic–ideally plastic for the purpose of analysis and is as follows:

$$\begin{aligned}\sigma_s &= E_s\varepsilon_s \quad 0 \leqslant \varepsilon_s \leqslant \varepsilon_y,\\ \sigma_s &= E_s\varepsilon_y \quad \varepsilon_y \leqslant \varepsilon_s,\end{aligned} \tag{2}$$

where σ_s and ε_s are stress and strain in steel rebars, respectively, E_s is the modulus of elasticity of steel and ε_y is the yield strain of steel.

The stress–strain relation of FRP composite plates is

$$\sigma_p = E_p\varepsilon_p, \tag{3}$$

where σ_p and ε_p are the average stress and strain in plates, respectively, and E_p is the modulus of elasticity of FRP.

3. Equilibrium of a bonded composite plate

To carry out numerical calculations, engineering approximations are used to model the bond between the concrete and FRP plate shown in Fig. 2. For the thin

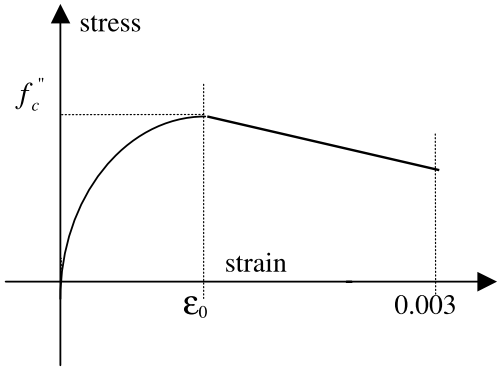

Fig. 1. Stress–strain relation of concrete.

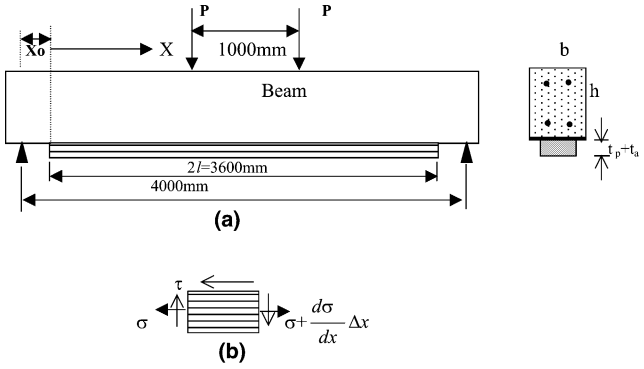

Fig. 2. Concrete beam reinforced by FRP plate. (a) FRP reinforced plate. (b) Equilibrium of a plate element.

adhesive layer, the shear strain at interface can be approximately calculated by

$$\gamma = \frac{u_c(x) - u_p(x)}{t_a}, \tag{4}$$

where u_c is the horizontal displacement of concrete at interface, u_p is the average displacement of FRP plate and t_a is the thickness of the adhesive layer. Hence, the shear stress at the interface is

$$\tau(x) = \frac{G_a[u_p(x) - u_c(x)]}{t_a}. \tag{5}$$

G_a here denotes shear modulus of the adhesive layer. Differentiation of shear stress with respect to x yields

$$\frac{d\tau(x)}{dx} = \frac{G_a}{t_a}(\varepsilon_p - \varepsilon_c^+) = \frac{G_a}{t_a}\left(\frac{\sigma}{E_p} - \varepsilon_c^+\right), \tag{6}$$

where ε_c^+ and ε_p are, respectively, the maximum tensile strain of concrete and the strain of the FRP plate at interface, and σ and E_p are, respectively, the longitudinal normal stress and elastic modulus of the plate. From Fig. 2(b), the horizontal equilibrium of the plate element can be written as

$$\frac{d\sigma(x)}{dx} = \frac{\tau(x)}{t_p}, \tag{7}$$

where t_p is the thickness of the plate. Eqs. (6) and (7) can be expressed by following first-order differential equation system in a matrix form:

$$\frac{d}{dx}\begin{Bmatrix}\sigma\\ \tau\end{Bmatrix} = \begin{bmatrix}0 & 1/t_p\\ G_a/E_p t_a & 0\end{bmatrix}\begin{Bmatrix}\sigma\\ \tau\end{Bmatrix} + \begin{Bmatrix}0\\ -G_a\varepsilon_c^+/t_a\end{Bmatrix}. \tag{8}$$

The general solution of the above equation can be represented by

$$\begin{Bmatrix}\sigma\\ \tau\end{Bmatrix} = \exp[\mathbf{K}x]\begin{Bmatrix}\sigma_0\\ \tau_0\end{Bmatrix} + \int_0^x \exp[\mathbf{K}(x-\xi)] \times \begin{Bmatrix}0\\ -G_a\varepsilon_c^+(\xi)/t_a\end{Bmatrix}d\xi, \tag{9}$$

where $\mathbf{K}$ is the 2×2 matrix in Eq. (8). σ_0 and τ_0 are the longitudinal normal and shear stresses at the cut-off edge ($x = 0$) of the plate (see Fig. 2). The exponential function of $\mathbf{K}x$ can be explicitly expressed as

$$\exp[\mathbf{K}x] = \begin{bmatrix} \cosh(\alpha x) & \sinh(\alpha x)/\alpha t_p \\ G_a \sinh(\alpha x)/\alpha E_p t_a & \cosh(\alpha x) \end{bmatrix},$$

$$\text{where } \alpha = \sqrt{\frac{G_a}{E_p t_p t_a}}. \tag{10}$$

Solution (9) can then be represented as

$$\begin{Bmatrix} \sigma \\ \tau \end{Bmatrix} = \begin{bmatrix} \cosh(\alpha x) & \sinh(\alpha x)/\alpha t_p \\ G_a \sinh(\alpha x)/\alpha E_p t_a & \cosh(\alpha x) \end{bmatrix} \begin{Bmatrix} \sigma_0 \\ \tau_0 \end{Bmatrix} + \int_0^x \begin{bmatrix} \cosh\alpha(x-\xi) & \sinh\alpha(x-\xi)/\alpha t_p \\ G_a \sinh\alpha(x-\xi)/\alpha E_p t_a & \cosh\alpha(x-\xi) \end{bmatrix} \times \begin{Bmatrix} 0 \\ -G_a \varepsilon_c^+(\xi)/t_a \end{Bmatrix} d\xi. \tag{11}$$

Due to the symmetry of the loaded beam (Fig. 2(a)) about its mid-span ($x = l$), the boundary conditions for the bonded plate are

$$\text{At } x = 0,\ \ \sigma_0 = 0 \quad \text{and} \quad \text{at } x = l,\ \ \tau = 0. \tag{12}$$

Introduction of Eq. (12) into (11) yields

$$\tau = \tau_0 \cosh(\alpha x) - \int_0^x \frac{G_a}{t_a} \cosh\alpha(x-\xi)\varepsilon_c^+(\xi)\,d\xi,$$
$$\sigma = \frac{\tau_0}{\alpha t_p} \sinh(\alpha x) - \int_0^x \frac{G_a}{\alpha t_a t_p} \sinh\alpha(x-\xi)\varepsilon_c^+(\xi)\,d\xi, \tag{13}$$

where

$$\tau_0 = \frac{1}{\cosh\alpha l} \int_0^l \frac{G_a}{t_a} \cosh\alpha(l-\xi)\varepsilon_c^+(\xi)\,d\xi. \tag{14}$$

From Eqs. (13) and (14), it is clear that the interfacial shear stress and the longitudinal normal stress of the plate depend on the variation of the maximum tensile strain at the bottom surface of the concrete beam.

The simple form solutions of Eq. (13) give explicit distributions of interfacial shear stresses and longitudinal normal stress in the composite plate. The solutions also provide an alternative benchmark result for finite element and other numerical analyses. It is a fact that the use of the finite element method is computational expensive and less reliable when material discontinuities are present. To model the singularity at the cut-off end of the plate, very fine finite element meshes have to be used to obtain a reasonably good solution. For non-linear problems where iterations are required, this solution becomes even more computational expensive. Using solution (13) when a linear modelling of concrete is acceptable, the ε_c^+ in Eq. (13) can be easily calculated on the basis of the simple beam theory. In most cases, ε_c^+ is a linear or quadratic function of x. Hence, the distributions of interfacial shear stress and the normal stress in composite plates can be found by calculating the integrals in Eqs. (13) and (14) analytically. For this special case, the solutions represented by Eq. (13) are identical to the linear form solutions obtained by [2]. If non-linear behaviour of concrete is preferred or complicate load conditions are considered, Eq. (13) may be used in two ways. The method can be used in conjunction with experimental methods. In real structures, the direct strains at bottom surfaces of a concrete beam can be measured easily by means of existing experiment techniques. The measured strains form an approximate distribution of ε_c^+ and the integrals in Eq. (13) can then be calculated. Alternatively, the distribution of ε_c^+ can be predicted analytically and the integrals are then calculated through an iteration process. The solution presented in this paper is for the analytical case and the iteration process is described in following sections.

4. Bending of a concrete beam reinforced with an external bonded FRP plate

The calculation of normal strain distribution of the reinforced concrete beam is based on the classic beam theory that assumes that: (a) the normal strain is distributed linearly across the thickness of the reinforced concrete beam, (b) the deformation is small, and (c) there is no shear deformation. The maximum compressive strain in the extreme fibre of concrete ε_{cmax} is taken as one of the parameters in the numerical calculation. Hence, the strains in the concrete, steel rebars and FRP plate can be represented, respectively, as follows [12]:

$$\varepsilon_c = \varepsilon_{cmax}(N - y)/N,$$
$$\varepsilon_s = \varepsilon_{cmax}(N - d)/N, \tag{15}$$
$$\varepsilon_p = \varepsilon_{cmax}(N - h - t_a - t_p/2)/N,$$

where N and d represent, respectively, the distance to the neutral axis of the cross-section and the steel rebars measured from the top concrete surface. When the yield strain occurs in the steel rebars, the corresponding value of N, N^*, can be calculated using the following equation:

$$N^* = E_s \varepsilon_{cmax} d/(E_s \varepsilon_{cmax} - \sigma_y), \tag{16}$$

where σ_y is the yield stress of steel.

For a given maximum compressive strain of concrete, ε_{cmax}, the axial forces F_c in concrete, F_s in steel rebars and F_p in FRP plate can be calculated, respectively, as follows:

$$F_c = \int_N^{h-N} E_c\varepsilon_c b\,dy - \int_0^N f_c''\left[\frac{2\varepsilon_c}{\varepsilon_0} - \frac{\varepsilon_c^2}{\varepsilon_0^2}\right] b\,dy$$
$$= E_c b\frac{(h-N)^2}{2N}\varepsilon_{cmax} - f_c'' bN\left[\frac{\varepsilon_{cmax}}{\varepsilon_0} - \frac{\varepsilon_{cmax}^2}{3\varepsilon_0^2}\right]$$
$$\text{for } 0 \leqslant \varepsilon_{cmax} < \varepsilon_0, \tag{17a}$$

$$F_c = \int_N^{h-N} E_c\varepsilon_c b\,dy - \int_{N\varepsilon_0/\varepsilon_{cmax}}^N f_c''\left[1 - \frac{0.15}{0.004-\varepsilon_0} \times (\varepsilon_c - \varepsilon_0)\right] b\,dy$$
$$= E_c b\frac{(h-N)^2}{2N}\varepsilon_{cmax} - \frac{f_c'' bN}{\varepsilon_{cmax}}\left\{\frac{2\varepsilon_0}{3} + (\varepsilon_{cmax} - \varepsilon_0) \times\left[1 - \frac{0.15}{0.004-\varepsilon_0}(\varepsilon_{cmax} - \varepsilon_0)\right]\right\},$$
$$\text{for } \varepsilon_{cmax} \geqslant \varepsilon_0 \tag{17b}$$

$$F_p = A_p E_p \varepsilon_{cmax}(h + t_a + t_p/2 - N)/N, \tag{18}$$

$$F_s = F_{st} + F_{sc}, \tag{19}$$

where

$$F_{st} = E_s A_{st}\varepsilon_{cmax}(d_{st} - N)/N,$$
$$F_{sc} = E_s A_{sc}\varepsilon_{cmax}(d_{sc} - N)/N, \quad \text{for } 0 \leqslant |E_s\varepsilon_s| < \sigma_y,$$
$$F_{st} = \sigma_y A_{st} \text{ for } \sigma_y \leqslant |E_s\varepsilon_{st}|,$$
$$F_{sc} = -\sigma_y A_{sc} \quad \text{for } \sigma_y \leqslant |E_s\varepsilon_{sc}|.$$

In the above equations, A_p is the cross-sectional area of the bonded composite plate, A_{st} and A_{sc} are the total cross-sectional areas of the steel rebars in tension and compression, respectively, d_{st} and d_{sc} denote the distances from the centres of these areas to the top surface of the beam, F_{st} and F_{sc} are, respectively, the tensile and compressive axial forces in steel while ε_{st} and ε_{sc} represent associated direct strains. In the calculation of F_c in Eqs. (17a) and (17b), the tensile strength of concrete (the first integral in the Eqs. (17a) and (17b)) is neglected when the tensile strain reaches the cracking strain of concrete. Otherwise, a linear elastic and uncracked section is assumed. The equilibrium of the internal axial forces over the cross-section provides a quadratic equation of N, by which the location of neutral axis can be obtained. For an assumed ε_{cmax}, an initial value of N is calculated by substituting Eqs. (17a), (17b), (18) and (19) into the following equilibrium equation,

$$F_c + F_s + F_p = 0. \tag{20}$$

The N obtained is then compared with N^* of Eq. (16). If N is larger than or equal to N^*, the location of the neutral axis has been found for the given ε_{cmax}. Otherwise N should be re-calculated using the forces at yielding in Eq. (21).

Once the location of neutral axis is found for the assumed ε_{cmax}, the bending moments on the cross-section, M_c, M_s and M_p, which are due to the axial stresses in concrete, steel rebars and FRP plate, respectively, are calculated as follows:

$$M_c = \int_0^{h-N} E_c\varepsilon_c b y\,dy - \int_0^N f_c'' b\left[\frac{2\varepsilon_c}{\varepsilon_0} - \frac{\varepsilon_c^2}{\varepsilon_0^2}\right] y\,dy$$
$$= \frac{E_c b(h-N)^3\varepsilon_{cmax}}{3N} + f_c'' bN^2\left[\frac{2\varepsilon_{cmax}}{3\varepsilon_0} - \frac{\varepsilon_{cmax}^2}{4\varepsilon_0^2}\right]$$
$$\text{for } 0 \leqslant \varepsilon_{cmax} < \varepsilon_0, \tag{21}$$

$$M_c = \int_0^{h-N} E_c\varepsilon_c b y\,dy + \int_0^{N\varepsilon_0/\varepsilon_{cmax}} f_c'' b\left[\frac{2\varepsilon_c}{\varepsilon_0} - \frac{\varepsilon_c^2}{\varepsilon_0^2}\right] y\,dy + \int_{N\varepsilon_0/\varepsilon_{cmax}}^N f_c'' b\left[1 - \frac{0.15}{0.004-\varepsilon_0}(\varepsilon_c - \varepsilon_0)\right] y\,dy$$
$$= \frac{E_c b(h-N)^3\varepsilon_{cmax}}{3N} + \frac{f_c'' bN^2}{\varepsilon_{cmax}^2}\left[\frac{5\varepsilon_0^2}{12} + \frac{1}{2}(\varepsilon_{cmax}^2 - \varepsilon_0^2) \times\left(1 + \frac{0.15\varepsilon_0}{0.004-\varepsilon_0}\right) - \frac{0.05}{0.004-\varepsilon_0}(\varepsilon_{cmax}^3 - \varepsilon_0^3)\right]$$
$$\text{for } \varepsilon_{cmax} > \varepsilon_0, \tag{22}$$

$$M_p = A_p E_p \varepsilon_{cmax}(h + t_a + t_p/2 - N)^2/N, \tag{23}$$

$$M_s = M_{st} + M_{sc}, \tag{24}$$

where

$$M_{st} = E_s A_{st}\varepsilon_{cmax}(d_{st} - N)^2/N,$$
$$M_{sc} = E_s A_{sc}\varepsilon_{cmax}(d_{sc} - N)^2/N, \quad \text{for } 0 \leqslant |E_s\varepsilon_s| < \sigma_y,$$
$$M_{st} = \sigma_y A_{st}(d_{st} - N) \quad |E_s\varepsilon_{st}| > \sigma_y,$$
$$M_{sc} = \sigma_y A_{sc}(d_{sc} - N) \quad |E_s\varepsilon_{sc}| > \sigma_y.$$

The total bending moment on the cross-section of the beam is then calculated by

$$M = M_c + M_s + M_p. \tag{25}$$

5. Calculation of ε_c^+

Due to the non-linear behaviour of concrete under compression, the location of neutral axis varies from section to section. To find the locations, an iterative method must be used. On an arbitrary cross-section of the beam, a ε_{cmax} is assumed so that the location of neutral axis is found on the basis of Eq. (21). The assumed ε_{cmax} and the neutral axis obtained is then used to find the bending moment on the section. The calculated bending moment is compared with the bending moment on the section, M_L, that is obtained by considering the equilibrium of the beam subjected to externally applied

loads. If $M < M_L$, a small increment is given to the assumed ε_{cmax}. Otherwise, a small decrement is given. The solution procedure is restarted from Eq. (21). The iteration finally yields the required ε_{cmax} and the location of neutral axis, from which the calculated bending moment on the cross-section is sufficiently close to the actual bending moment on the section due to the external loads. In general, different load cases (except for pure bending) lead to different moment distributions along the beam. As a result, the location of neutral axis and ε_{cmax} vary along the beam. From Eq. (15), The distribution of ε_c^+ can be calculated on the bases of the ε_{cmax} and N obtained and brought into the integrals in Eqs. (13) and (14) to find the distribution of interfacial shear stress.

6. Numerical test and results

Numerical calculations were carried out for rectangular concrete beams reinforced by steel rebars and bonded composite plates. The beams have the following geometrical and material properties (unless stated otherwise):

(a) concrete

$b = 200$ mm, $h = 400$ mm, $E_c = 27990$ MPa,

$f'_c = 34.32$ MPa, $\zeta = 0.85$.

(b) steel

$E_s = 200$ GPa, $\sigma_y = 456$ MPa,

$A_{st} = A_{sc} = 265$ mm^2,

(c) adhesive layer (glue)

$G_a = 297$ MPa, $t_a = 2$ mm,

(d) composite plate

$E_p = 37230$ MPa, $t_p = 6$ mm.

Figs. 3 and 4 show the distributions of the interfacial shear stress and the longitudinal normal stress of the FRP near the cut-off end of the bonded plate. The beam is symmetrically loaded as shown in Fig. 2 with $P = 100$ KN. The beam was also analysed by using the finite element method. Four-node 2D plane stress elements were used in the analysis. As a special case, the solutions for linear concrete were also obtained and they are identical to the ones presented by [2]. It can be seen from the figures that the stress distributions predicted by using present method are in good agreement with those obtained by using the FE method. All the results show significant shear stress concentration at the cut-off end, from where the stress decays away rapidly.

Figs. 5 and 6 show, respectively, the shear stress distributions near the cut-off end of the plate for different plate materials, E_p, and the thickness of the adhesive layer, t_a. From Fig. 5, it is clear that an increase of E_p increases the level of shear stress almost uniformly over the distance. From Fig. 6, however, it is observed that a variation of the thickness only alternates the distribution of shear stress significantly over a very short distance away from the cut-off end.

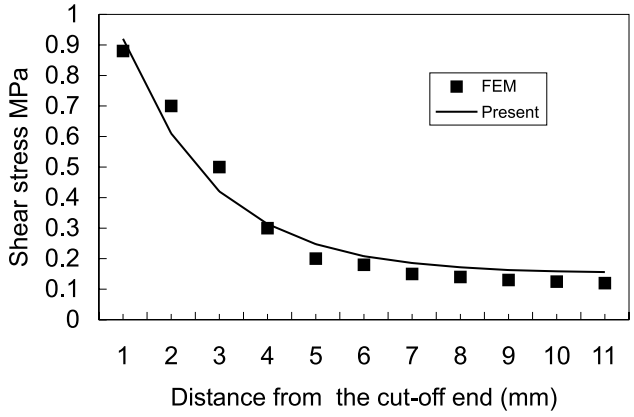

Fig. 3. Shear stress near the cut-off end.

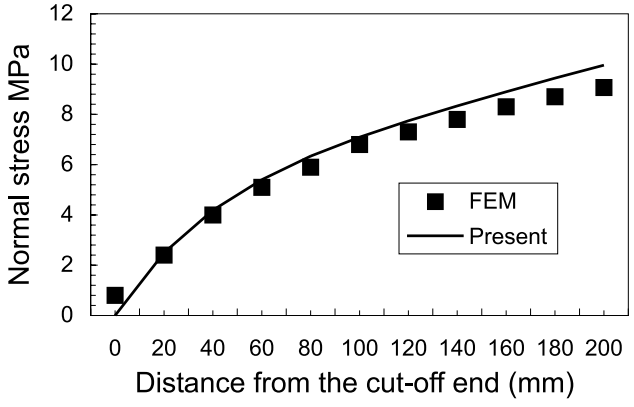

Fig. 4. Distribution of longitudinal normal stress in FRP plate.

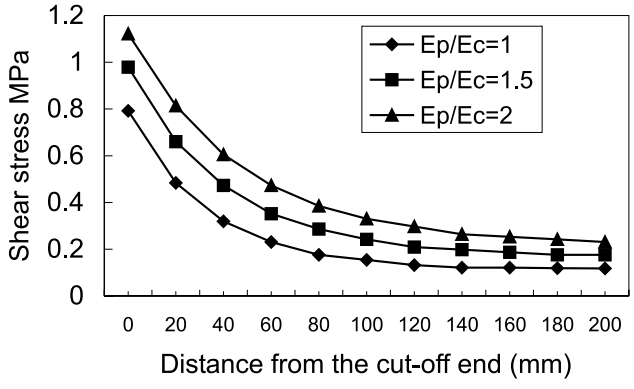

Fig. 5. Shear stress near the cut-off end viz. E_p.

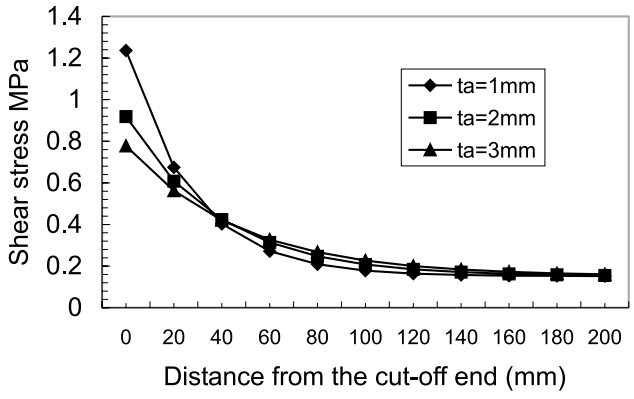

Fig. 6. Shear stress near the cut-off end viz. t_p.

Figs. 7 and 8 are the corresponding results for the longitudinal normal stress in the FRP plate when either the material property of plate or the thickness of adhesive layer varies. The same observations as those observed from Figs. 5 and 6 for shear can also be made for longitudinal normal stresses.

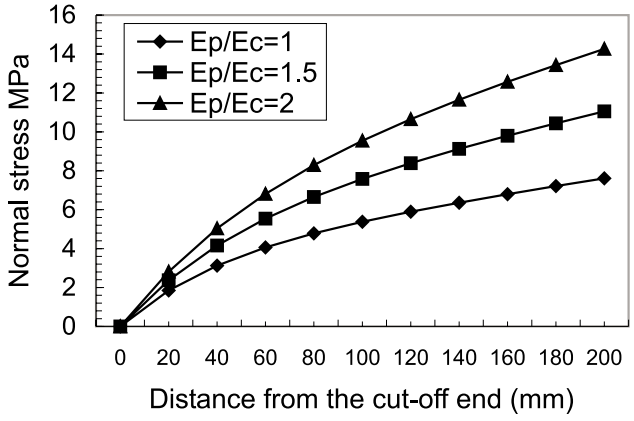

Fig. 7. Longitudinal normal stress in FRP plate viz. E_p.

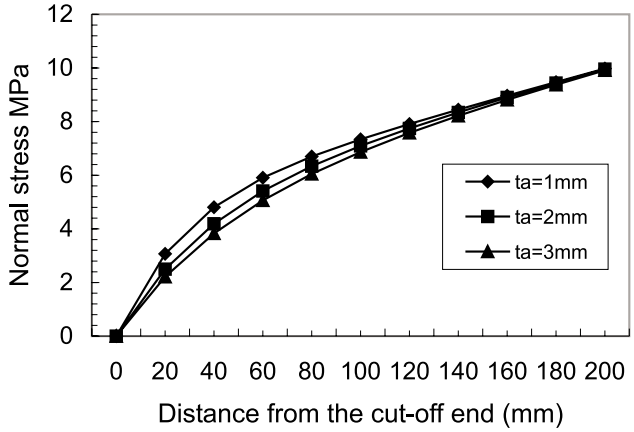

Fig. 8. Longitudinal normal stress in FRP plate viz. t_a.

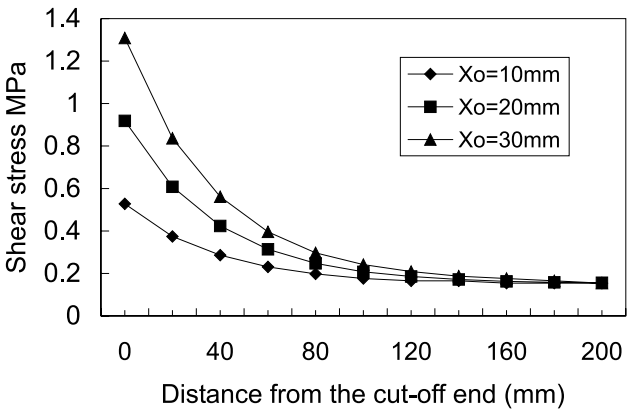

Fig. 9. Shear stress near the cut-off end viz. X_0.

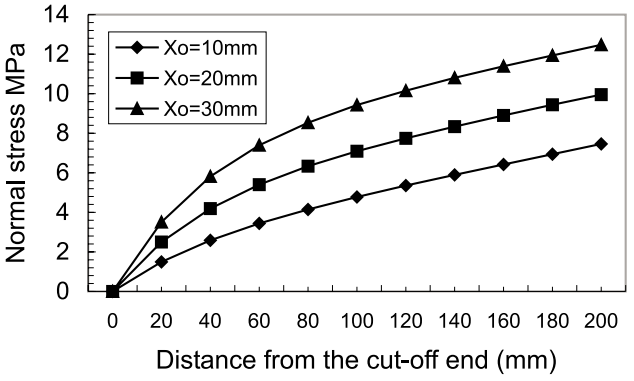

Fig. 10. Longitudinal normal stress in FRP plate viz. X_0.

Figs. 9 and 10 present, respectively, the shear stress and the longitudinal normal stress near the cut-off end of the plate for three cases where the FRP plate is terminated at various distances (X_0) from the support. It is clear that both shear and longitudinal stresses increase as the distance becomes longer. For shear stress, it is noticed that only in the region near the cut-off end, the shear stress increases significantly.

7. Concluding remarks

An analytic method has been proposed to investigate the shear transfer at the interfaces of concrete beams reinforced by bonded FRP plates. The non-linear properties of concrete under compression has been considered.

Numerical solutions obtained by using present method were compared with those obtained from alternative methods. The possibility of using present method in conjunction with experimental approaches was discussed.

Significant shear stress concentration was observed at the cut-off end of the FRP plate. Further numerical re-

sults showed that the shear stress near the cut-off end increases when (a) a thinner adhesive layer is used, (b) a stiffer (high modulus) FRP plate is used and (c) the FRP plate is terminated at a longer distance from the support.

It has been observed that any alternation of the design variables discussed in the paper only affect shear stress distribution significantly over a short distance from the cut-off end of the bonded plate.

Further research is needed to deal with the presence and propagation of cracks in concrete. The shear concentration at crack openings towards the overall distribution of interfacial shear stress should also be considered.

References

[1] Demers M, Neale KW. Confinement of reinforced concrete columns with fibre reinforced composite sheets – an experimental study. Can J Civil Eng 1999;26(2):226–41.

[2] Malek AM, Saadatmanesh H, Ehsani MR. Shear and normal stress concentration in RC beams strengthen with FRP plates. In: Proc Adv Compo Mat Bridges Struct. Montreal, Canada; 1996. p. 629–37.

[3] Meier U. Bridge repair with high performance composite materials. Mater Technik 1987;4:125–8.

[4] Niterekac C, Neale KW. Analysis of reinforced concrete beams strengthened in flexure with composite laminates. Can J Civil Eng 1999;26(5):646–54.

[5] Park R, Pauley. Reinforced concrete structures. New York: Wiley; 1975.

[6] Quantrill RJ, Hollaway LC, Thorne AM. Experimental and analytic investigation of FRP strengthened beam response: Part I. Mag Concr Res 1996;48(177):331–42.

[7] Saadatmanesh H, Ehsani MR. RC beams strengthened with GFRP plates. J Struct Eng 1991;117(11):3417–33.

[8] Swamy R, Gaul. Repair and strengthening of concrete members with adhesive bonded plate. ACI SP-165, USA; 1996.

[9] Triantafillou TC, Deskovic N. Innovative prestressing with FRP sheets: mechanics of short-term behavior. J Eng Mech, ASCE 1991;117(7):1652–72.

[10] Triantafillou TC, Deskovic N, Deuring M. Strengthening of concrete structures with prestressed fiber reinforced plastic sheets. ACI Struct J 1992;235–44.

[11] Wei An, Saadatmanesh H, Ehsani MR. RC beams strengthened with FRP plates. J Struct Eng 1991;117(11):3434–55.

[12] Ye JQ. Interfacial effects on RC beams strengthen by bonded composite plates. In: Proc 2nd Asian–Pacific Speciality Conf Fibre Reinforced Concr; 1999. p. 235–42.